Journal of Analytical and Applied Pyrolysis 173 (2023) 106100

Contents lists available at ScienceDirect

Journal of Analytical and Applied Pyrolysis

journal homepage: www.elsevier.com/locate/jaap

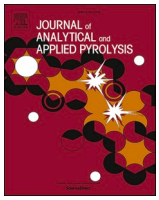

Recovery of styrene-rich oil and glass fibres from fibres-reinforced unsaturated polyester resin end-of-life wind turbine blades using pyrolysis technology

Samy Yousef [a,*], Justas Eimontas [b], Kęstutis Zakarauskas [b], Nerijus Striūgas [b]

[a] Department of Production Engineering, Faculty of Mechanical Engineering and Design, Kaunas University of Technology, LT-51424 Kaunas, Lithuania
[b] Lithuanian Energy Institute, Laboratory of Combustion Processes, Breslaujos 3, LT-44403 Kaunas, Lithuania

ARTICLE INFO

Keywords:
End-of-life wind turbine blades
Glass fibres-reinforced unsaturated polyester resin
Pyrolysis
Styrene
Recycled short fibres

ABSTRACT

Styrene is the main compound of unsaturated polyester resin (UPR) of end-of-life wind turbine blades (WTBs) with high toxicity. This research aims to recover styrene and glass fibre (GF) from WTBs composed of GF/UPR using a small pyrolysis plant with a reactor capacity of 250 g. The conversion process was carried out at 25 °C/min at different pyrolysis temperatures: 500, 550 and 600 °C to obtain the optimal temperature at which each UPR fragment can decompose while maintaining the morphology of the recovered GF. The produced gases were monitored during the entire conversion process of WTBs using an instantaneous gas analyzer. The pyrolysis products (oil and gaseous) derived at the end of the process were analyzed using gas chromatography-mass spectrometry (GC/MS). Char and short GF in solid residual products were separated using a sieving process, followed by washing and analysis of their chemical structure and morphology using Fourier-transform infrared spectroscopy, a scanning electron microscope, and an optical microscope. The results showed that at 500°C, WTBs was converted into oil (44.5 %) and solid residues (55 %), while very little amount of gas could be neglected. Also, styrene (upto 48.53 %) was the major compound in the GC/MS analysis of oil product and CO_2 was the main gas in gaseous product. However, the recovered GF was still loaded with UPR debris on its surface, which could crack at 600 °C without affecting surface of the recovered GF. Meanwhile, potassium was the major element in char products with concentration in the ranges of 14.9 wt% (500 °C) - 25.5 wt% (600 °C).

1. Introduction

In light of the current massive consumption rate of wind energy, which has reached 743 GW [1], end-of-life wind turbine blades (WTBs) have emerged as a new challenge for those responsible for this industry and those concerned with environmental issues that need a quick and effective treatment, especially as it is expected that this consumption rate will increase up to 5270 GW (onshore and offshore) by 2050 [2]. Also, these blades have short lifecycle ranges between 20 and 25 years and it is expected that more than 4.3×10^7 tons of WTBs will be produced by 2050 [3]. All these facts were a strong motivation for decision makers to pump more investments into invention of new technologies that would replace landfills and take advantage of this huge wealth through their recycling [4]. This buried or wasted wealth has a composite structure consisting primarily of fabrics (made of glass or carbon fibres) and resins (e.g, polyester, epoxy, etc.). Besides, some thermoplastic coatings and other adhesives are extremely difficult to recycle [5,6]. Despite this complexity in their structure, there could be found many attempts in the literature to recycle them using various mechanical, chemical, and thermal processes [7]. Mechanical recycling is usually used to grind WTBs into smaller parts, which can then be used as filler in production of building composite materials [8,9]. However, due to emitted dust and smaller compatibility of these fillers and cement, less composites with mechanical performance and low market value are generated. Moreover, in recycling field, mechanical process is defined as a pre-treatment process used for size reduction and not as a customary main treatment [10]. Meanwhile, chemical processing has many occupational health and safety concerns due to its main reliance on separating the resin fraction using various organic solvents and some of them are very toxic with high potential environmental impact [11,12]. Although this process succeeded to recover fibre materials, resin lost some of its properties, including mechanical and chemical structure

* Corresponding author.
E-mail address: ahmed.saed@ktu.lt (S. Yousef).

https://doi.org/10.1016/j.jaap.2023.106100
Received 14 June 2023; Received in revised form 24 July 2023; Accepted 26 July 2023
Available online 27 July 2023

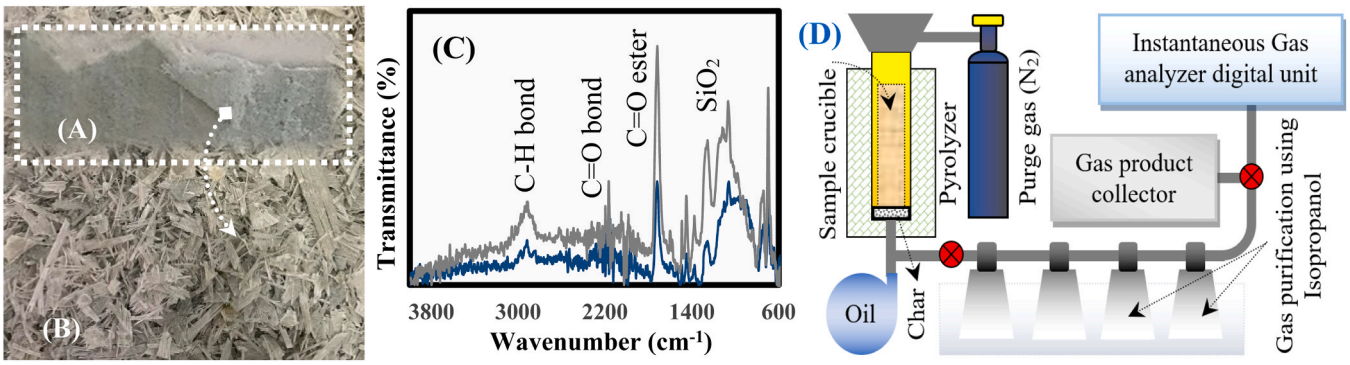

Fig. 1. A) Image of the supplied WTBs, B) shredded WTBs, C) FTIR of WTBs, and D) scheme of the pyrolysis experimental setups.

[13]. Also, this approach has been used to treat waste printed circuit boards that have a composition similar to that of WTBs, however, it has not been applied for WTBs so far due to the toxic concerns and economic considerations. On the other hand, thermal recycling process, including gasification and pyrolysis, can be used to decompose the organic components of WTBs thermally into carbonaceous components (oil and syngas) with high calorific values [14,15]. Through the gasification process, the resin can be decomposed into hydrogen-rich synthesis gas, however, this process is very risky as it must be performed under pressures as high as 40 MPa, in addition to its hard setup, high temperature, and pressure at industrial scale [16]. To the contrary, pyrolysis is quite simple and inexpensive, when compared to gasification process, where resin (thermosetting and thermoplastic) can be decomposed in presence of nitrogen into oil, or commodity chemical products, gas, and residues at 500 °C [17–19]. The studies also showed that this process is highly sensitive to operating parameters (reaction temperature and heating rate), as it is possible to improve the composition and yield of pyrolysis products by controlling these parameters and involving a catalyst in the reaction in different proportions [20–24]. In addition, the catalyst can help to reduce the reaction activation energy and complexity of the reaction even with a change in the type of adhesive material of WTBs [25,26]. All these results made pyrolysis a promising candidate for energy and fibre recovery from WTBs with high environmental and techno-economic performances [27,28].

Although these results of WTBs pyrolysis are promising, but majority of them were presented as a systematic overview based on different feedstocks with a structure similar to WTBs, such as fibre-reinforced polymer composites, and only few studies focused on the commercial WTBs having a glass fibres/poxy composition [17]. Besides, in most of these studies the pyrolysis process was performed using thermogravimetric analysis with a few milligrams of feedstock, basic information about the characteristics of various pyrolytic products and their thermal degradation kinetics [20–23], what makes it difficult to correctly explore the final yield and its economic aspects and environmental performance. Also, it was difficult to characterize different pyrolysis products as the main energy product generated was in the form of vapour phase. In addition, most of these studies focused on epoxy resin, while other resins such as unsaturated polyester resin (UPR) are still left unexamined [29]. Generally, the consumption rate of UPR in blade production lower than epoxy resin and unfortunately no specific statistics are available on this subject [30,31], where the blade composition is proprietary to each manufacturer, making it difficult to obtain such these percentages and the real composition. However, UPR mainly contains styrene, which is classified as a highly toxic and air pollutant (according to European Chemical Agency and US Environmental Protection Agency [32,33]) and its recovery can be protect our planet. Also, it is expected by 2034, more than 225,000 tons of WTBs will be recycled annually worldwide [34]. This situation necessitates the development of industrial solutions for its recycling.

Hydrolysis is one such advanced solution that has recently been used to decompose UPR and its compounds in alkaline environments [31,35]. Although this method was successful in cleaving ester bonds in UPRs and separate fibres, however, this approach is usually performed in the presence of a catalyst such as metallic salt soluble and chemicals (e.g., hydrazine, sodium hydroxide, sulfuric acid, hydrogen peroxide, ferrous sulfate, etc.) in water which results in the production of secondary chemical waste that need to be carefully disposed or treated, especially as some are toxic [36]. Also, the experiments were carried out at small or fundamental scale what needs more researches for upscaling. On contrary, pyrolysis is characterized by its simplicity without almost producing almost any further waste. Also, the pyrolysis behaviour of UPR and their composites (E-glass fiber/UPR) were studied in the literature using thermogravimetric analyzer (TGA) [37,38]. However the thermal decomposition of commercial WTBs composed of GF/UPR structure still missing, especially, the commercial WTBs have a very thin coating layer (gelcoat) made of different organic components used to protect the surface of blades from erosion and wear during operation in harsh weather [39], which can affect composition of the formulated oil and its decomposition mechanism. In addition, due to long operation in harsh weather conditions, WTBs degenerate (e.g., hygrothermal aging) [40,41]. In order to explore this, this paper aims to investigate potential applications of pyrolysis treatment in recycling of commercial WTBs composed of glass fibre (GF)/UPR composites. The experiments were carried out on commercial WTBs samples using a small pyrolysis plant at various temperatures. The yield and properties of the recovered energy, GF, and char products were calculated and examined. This study presents effective solutions that ensure preservation of resources for future generations and make the wind energy sector greener. Besides, the present research was carried out by a complete transformation system similar to the industrial level which helps to scale up and obtain more accurate results.

2. Experimental

2.1. Materials and feedstock preparation

The WTBs feedstock (GF/UPR) in the form of small pieces was supplied by European Energy, Denmark, as shown in Fig. 1**A** and the virtual shape of WTBs debris consisting of fibrous bundles is shown in Fig. 1**B**. Depending on the supplier of WTBs, the feedstock is mainly GF and UPR. To confirm this, the raw material was analyzed again using FTIR to clarify its composition and the results are shown in Fig. 1**C**. The analysis was performed on resin polymer part only, while the FTIR of fibres part shown in Section 3.5 as a recovered GF. FTIR spectra of the resin polymer were performed in two batches collected from different locations. The analysis showed several peaks at 700–760 cm^{-1} (aromatic bonds C–H), 890–1255 cm^{-1} (bending modes of SiO_2), 1448 cm^{-1} (carbonyl group), 1716 cm^{-1} (C═O ester), 2169 cm^{-1} (C═O bond), 2913 cm^{-1} (C-H bond). Among these peaks, SiO_2 (related to GF) and C═O ester represents the major functional groups of UPR [42]. While

Table 1
Yields distribution of pyrolysis of WTBs products at various temperatures.

Pyrolysis product	500 °C	550 °C	600 °C
Oil (wt%)	44.54	41.39	39.45
Solid residue (wt%)	55.03	58.02	60.42
Gaseous (wt%)	0.43	0.59	0.13

the other peaks corresponding to the groups of the remaining elements form coating layer and fibreglass. Based on elemental analysis of the organic part of GF/UPR, the sample composed of nitrogen (< 0.01 wt%), carbon (61.091 wt%), hydrogen (4.224 wt%), sulfur (< 0.01 wt%), and oxygen (34.685 wt%). While proximate analysis showed that the sample was rich in volatile matter (87 wt%) beside few contents of fixed carbon (9.9 wt%) and ash (2.43 wt%) and moisture (0.64 wt%). As shown in the results, the sample contains less hydrogen which can reduce the amount of water in the processed products. Finally, the supplied WTBs were exposed to additional mechanical pretreatments, such as shredding and grinding processes, to reduce their size, which helps to increase their surface-to-volume ratio and thus, to accelerate heat transfer during the reaction [43].

2.2. Pyrolysis setups used for recycling of WTBs

The pyrolysis experiments of WTBs with GF/UPR composition were carried out using a lab-scale setup and its components are described in Fig. 1**D**. The setup consists of pyrolyzer, gas purification using isopropanol, and instantaneous gas analyzer digital (IGAD) unit. The experiments were started with heating the reactor and removing oxygen from inside by pumping nitrogen (N_2) for 20 min followed by addition of 250 g of WTBs feedstock in the pyrolysis crucible at various reaction temperatures of 500, 550, and 600 °C. These heating conditions were kept until the resin part of WTBs decomposed completely into oil and gaseous products. The total reaction time took 45–77 min (depending on the pyrolysis temperature). The experiments were conducted at a N_2 flow rate of 60 mL/min and heating rate of 20 °C/min. These thermal degradation conditions were selected based on the optimal conditions received from thermogravimetric and gas chromatography-mass spectrometry (GC/MS) results manifesting complete decomposition of the WTBs samples and the maximum amount of volatile compounds in the

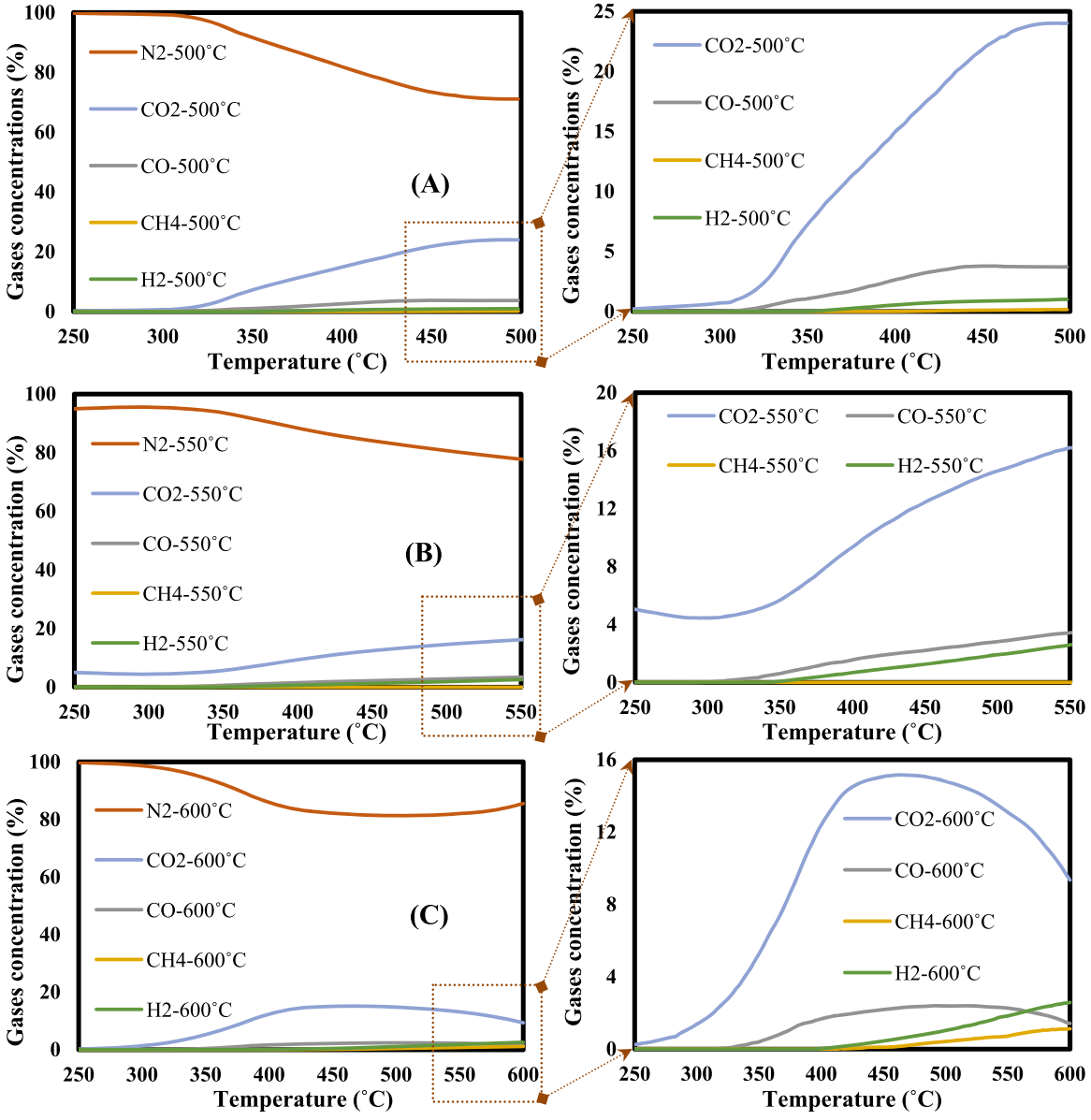

Fig. 2. Distributions of the generated gases at A) 500 °C, B) 550 °C, and C) 600 °C.

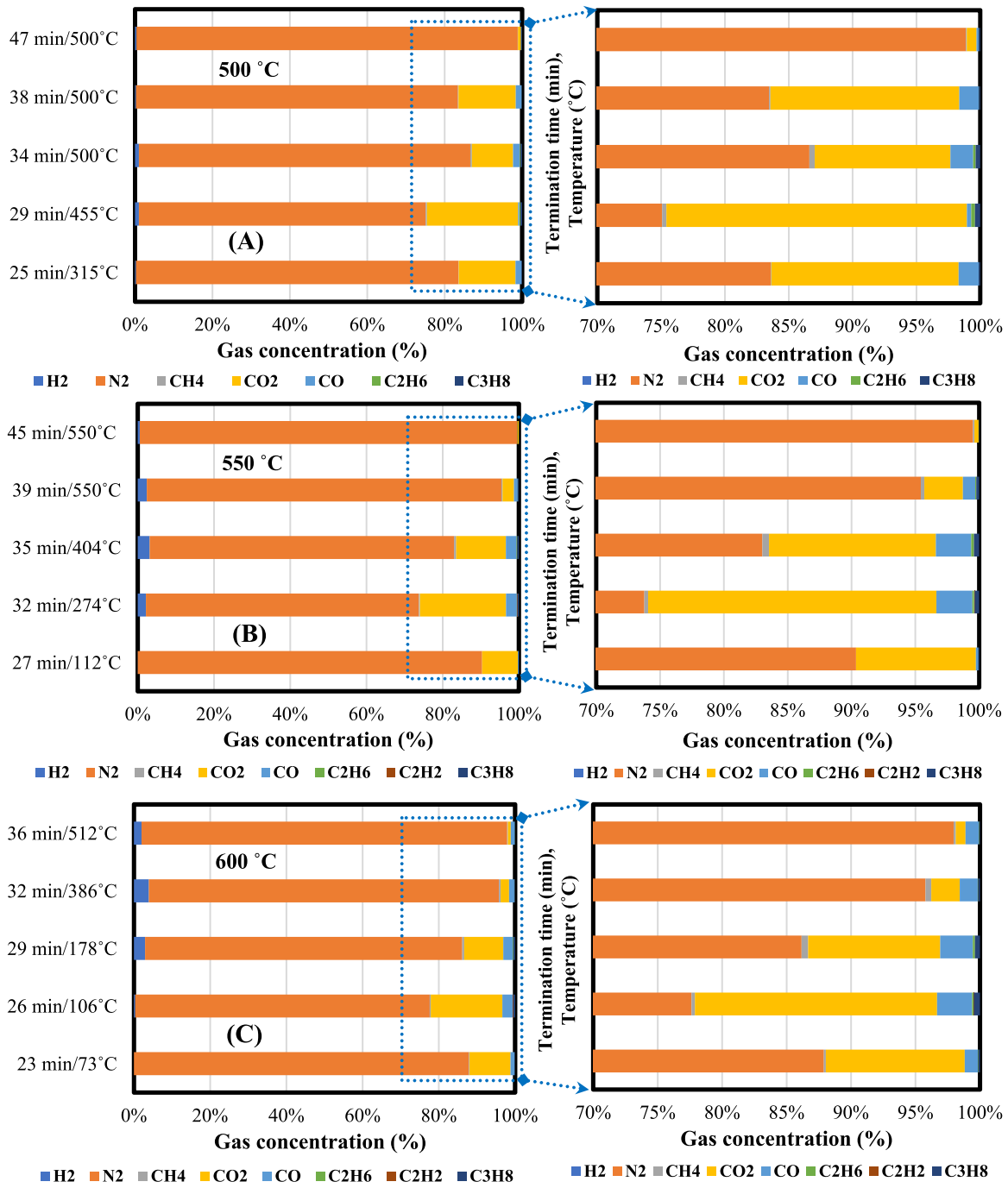

Fig. 3. GC-TCD analysis of composition of the gases produced from pyrolysis of WTBs at different temperatures (500, 550, and 600 °C).

pyrolysis vapour products [20–23]. The obtained liquid product (Fig. 4) has a low viscosity that reduces the possibility of its adhesion to the inner surface of the pipes. Also, under the action of gravity, this heavy oil leaves the reaction chamber and passes through the vertical piping system to be collected in the liquid product collector (glass vessels). While the gases with light density passed in the horizontal piping system for purification, analysis, and collection. Meanwhile, the recovered fibres containing char residues on their surface remained as a mixture at the bottom of the reactor. They could be taken out of the reactor after cooling followed by careful separation of fibres from solid residues using a sieving process, then washing them with deionized water.

2.3. Characterizations of pyrolysis products

The composition of gaseous products generated during pyrolysis of WTBs was recorded using the conversion process with an IGAD unit (Zambelli - Model ZB1). Agilent 7890 A gas chromatograph-dual-channel thermal conductivity detectors (GC-TCD) were used to analyze the obtained gas devoid of any condensable substances. Whereas, the liquid products obtained from pyrolysis of WTBs under the specified treatment conditions were characterized using GC/MS (Shimadzu GC-2010). Finally, the morphology and chemical structure of the recovered fibre bundles and char residues were analyzed using Fourier-transform infrared spectroscopy (FTIR), Scanning electron microscope (SEM)- Energy-dispersive X-ray (Model BPI-T), and an optical microscopy.

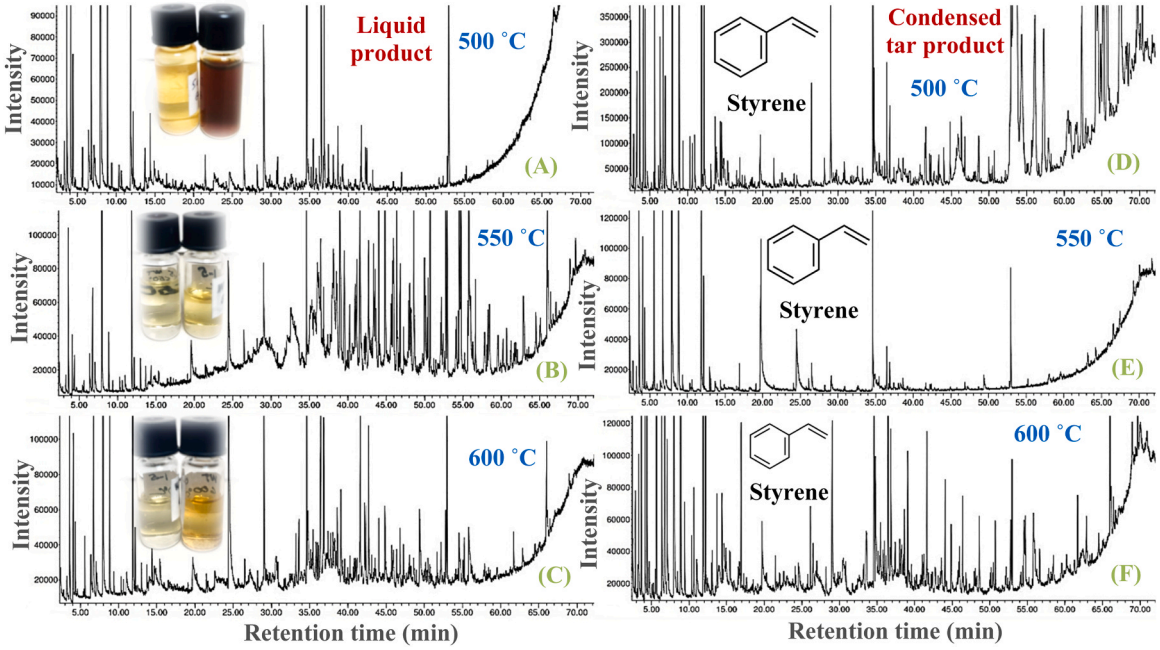

Fig. 4. GC/MS of A-C) oily products and D-F) Condensed tar product recovered from WTBs.

3. Results and discussion

3.1. Yields and distribution of pyrolysis products

Once the WTBs treatment had been completed using mechanical and pyrolysis processes, the formulated products (gaseous, oil, and solid residues) were collected after each run (500, 550, and 600 °C), followed by calculation of their yield based on the weight balance and the estimated yields are illustrated in Table 1. As shown, the maximum oil yield was obtained at 500 °C and its yield decreased with increasing temperature due to the increase in the rate of oil cracking into gases, evaporation into a gaseous phase. The molecules of these gases split up to form flakes of solid carbon under the applied high temperature [44]. Also, this is the main reason why the yield of gaseous and solid residue products took opposite direction, where their yield increased as temperature was increasing. This can enhance decomposition process and generate more chemical reaction rates of the liquid phase to vapourize and convert gas phase [45,46]. However, these results can be deceptive because the proportion of fibre in the feedstock is not easily controlled and can change from batch to batch. Thus analysis and characterization of the obtained pyrolysis products can help in determining the optimum pyrolysis temperature.

3.2. Effects of pyrolysis temperature on gases distribution

Fig. 2 shows the distribution of all generated gases (N_2, CO_2, CO, CH_4, H_2) and their concentration during the entire conversion process from room temperature until the end of reaction within the specified temperatures (500, 550, and 650 °C). The IGAD measurements showed that the conversion process of WTBs started at ambient N_2 devoid of other gases up to 300 °C, which means that treatment was conducted based on the standard thermochical protocols [47]. After this temporary stability in the agent ambient composition, CO_2, CO, H_2, CH_4, and CO gases began to be emitted and participate in the reaction leading to gradual decrease of N_2 amount [48]. Then, in the last phase of the reaction, they became a little more stable. Meanwhile, the analysis of the gases emitted from decomposition of WTBs showed that CO_2 was the most predominant gas in the synthised gases with abundance of 24 % (500 °C), 16 % (550 °C), and 15 % (600 °C). It was learnt that concentration of CO_2 decreases with increasing temperature [49]. Also, CO_2 concentration decreased up to 9 % at higher temperature, hence contributing to its decomposition into other compounds. Also, it was observed that CO_2 gas generated at 550 °C started a little early compared to the other batches, and the composition of the raw materials may have been slightly different and loaded with more coat layer and organic components that have lower thermal stability than other components, which leads to an early onset of CO_2 gas. Other gases showed very small abundances below 3.7 %. However, such type of measurements cannot be used to detect light hydrocarbon compounds such as C_2H_6 and C_3H_8 and thus, a methane cell detector was used to deal with these gases CH_4 [50,51].

Therefore, the gaseous products generated at the specified conditions were collected using portable constant flow sampler at various reaction times to cover the majority of degradation phases; then they were characterized by a GC-TCD that can be used to identify these gases and the results are displayed in Fig. 3. The measurements showed that, as the pyrolysis temperature increased, the reaction time (termination time) required for decomposition of all WTBs was also increasing, where termination time was estimated at 54 min (500 °C), 62 min (550 °C), and 77 min (600 °C). These big differences in termination times made it difficult to collect the tested gas samples at the same reaction time for all WTBs samples. As shown, the reaction agents (N_2) and CO_2 were the predominant gases together with other light hydrocarbons, such as CH_4, C_2H_6 and C_3H_6 gases, especially at higher temperature, what means that the generated gases were loaded with other compounds. However, this amount of gases is very small and it can be disposed of by burning. It seems that at some point the rate of heating is not constant in different temperature conditions and this is not true and this discrepancy is due to the fact that the temperature has been raised to the specified value (500 °C or 550 °C or 600 °C), then it remains constant until the measured gases show zero values.

3.3. GC analysis of liquid products

Fig. 4 shows GC/MS analysis of the collected oily products and condensed tars resulted from pyrolysis of WTBs at 500, 550, and 600 °C, and their real images. The GC/MS spectrum of oil products **(Fig. 4A-C)** shows several peaks, such as toluene, styrene, benzene, 1,1′-(1,3-

Table 2
GC/MS of distribution of oily products recovered at various temperatures.

500 °C			550 °C			600 °C		
Time (min)	GC Compounds	Area (%)	Time (min)	GC Compounds	Area (%)	Time (min)	GC Compounds	Area (%)
3.322	Acetic acid, (2-propenylthio)-	0.54	3.270	2-Isopropoxyethylamine	0.32	3.270	Phloroglucitol	0.50
3.645	Toluene	4.10	3.594	Toluene	1.72	3.574	Toluene	2.83
4.143	1,3-Dioxolane, 2-ethyl-4-methyl-	2.48	4.105	Hydrazine, 1,1-diethyl-2-(1-methylpropyl)-	0.88	4.072	1,3-Dioxolane, 2-ethyl-4-methyl-	1.86
4.402	1,3-Dioxolane, 2-ethyl-4-methyl-	1.10	4.350	Hydrazine, 1,1-diethyl-2-(1-methylpropyl)-	0.45	4.338	1,3-Dioxolane, 2-ethyl-4-methyl-	0.85
5.670	Propane, 2,2′-[ethylidenebis (oxy)] bis-	0.36	6.394	2-Propanol, 1-(2-propenyloxy)-	0.75	5.599	Propane, 2,2′-[ethylidenebis (oxy)] bis-	0.60
6.485	2-Propanol, 1-(2-propenyloxy)-	1.14	6.737	Ethylbenzene	1.47	6.414	2-Propanol, 1-(2-propenyloxy)-	0.91
6.783	Ethylbenzene	3.23	7.080	Methacrylamide	0.68	6.731	Ethylbenzene	2.66
7.158	2-Butanol, 1,4-dimethoxy-3-(1,2,2-trimethylpropoxy)-	0.60	7.934	Styrene	19.89	7.093	Methacrylamide	0.65
7.966	Styrene	48.53	8.846	2-Hexanol, 2-methyl-	0.69	7.928	Styrene	29.77
8.885	2-Hexanol, 2-methyl-	1.65	10.987	Benzaldehyde	0.29	8.840	Propane, 1,2,3-trimethoxy-	2.04
10.392	Benzene, 2-propenyl-	0.35	11.841	.alpha.-Methylstyrene	2.62	11.078	Benzaldehyde	0.45
11.874	.alpha.-Methylstyrene	6.89	12.158	Heptane, 2,2,4,6,6-pentamethyl-	0.36	11.848	.alpha.-Methylstyrene	4.37
12.178	Heptane, 2,2,4,6,6-pentamethyl-	0.66	12.973	Cyclotetrasiloxane, octamethyl-	0.39	12.158	Heptane, 2,2,4,6,6-pentamethyl-	0.61
13.749	Benzene, 1-ethenyl-2-methyl-	0.63	13.678	Benzene, 2-propenyl-	0.34	19.720	Benzoic acid	0.76
21.505	Benzene, 1-hexynyl-	0.35	19.597	Benzoic acid	0.70	24.455	Phthalic anhydride	13.50
22.650	N-Isopropyl-3-phenylpropanamide	0.35	24.494	Phthalic anhydride	2.97	29.041	Dimethyl phthalate	2.72
26.525	Biphenyl	0.71	29.041	Dimethyl phthalate	1.28	34.604	Benzene, 1,1′-(1,3-propanediyl) bis	8.58
28.226	Diphenylmethane	0.34	34.611	Benzene, 1,1′-(1,3-propanediyl) bis	4.76	36.454	3-Benzyl-5-chloro-1,2,3-triazole 1-oxide	3.42
29.087	Dimethyl phthalate	2.45	38.996	Tetradecanal	6.27	36.855	1,2-Diphenylcyclopropane	1.99
34.611	Benzene, 1,1′-(1,3-propanediyl) bis	10.50	41.590	Oxirane, hexadecyl-	6.36	39.100	Oxirane, tetradecyl-	1.17
35.465	Benzene, 1,1′-(1-methyl-1,3-propanediyl)bis-	0.50	42.716	n-Hexadecanoic acid	2.60	41.636	Phthalic acid, cyclohexylmethyl isohexyl ester	2.11
36.241	(*E*)-Stilbene	0.47	44.029	Oxirane, hexadecyl-	4.35	42.186	Phthalic acid, cyclohexylmethyl ethyl ester	0.96
36.474	3-Benzyl-5-chloro-1,2,3-triazole 1-oxide	3.27	44.838	4,4′-(Hexafluoroisopropylidene) diphenol	7.87	42.341	1,4-Dioxo-1,2,3,4-tetrahydrophthalazine	1.01
36.862	1,2-Diphenylcyclopropane	1.93	46.364	17-Octadecenal	4.31	42.722	n-Hexadecanoic acid	2.10
38.059	Benzene, 1,1′-(3-methyl-1-propene-1,3-diyl)bis-	0.38	46.811	Cyclodecasiloxane, eicosamethyl-	1.85	44.048	Pentadecanal-	0.53
38.647	Benzene, 1,1′-(3-methyl-1-propene-1,3-diyl)bis-	0.63	48.602	Bicyclo[10.8.0]eicosane, cis-	4.05	44.870	4,4′-(Hexafluoroisopropylidene) diphenol	0.87
41.662	2-Hydroxy-1-isoindolinone	0.73	49.980	Cyclononasiloxane, octadecamethyl-	1.34	47.283	dl-Phenylephrine	0.43
42.192	2-Hydroxy-1-isoindolinone	0.40	50.472	1,3,2-Oxazaborolane, 2-butyl-	1.33	49.430	1,8-Diazacyclotetradecane-2,9-dion	2.42
42.367	4-Methyl-6-phenyltetrahydro-1,3-oxazine-2-thione	0.53	50.724	Octadecanal	3.33	52.788	(+)-N-Benzyl-.alpha.-phenethylamin	0.76
52.956	1,2-Propanediol, 3-benzyloxy-1,2-diacetyl-	4.22	52.768	1,21-Docosadiene	2.49	52.956	1,2-Propanediol, 3-benzyloxy-1,2-diacetyl-	6.94
			54.379	2-Tetradecanone	0.68	54.560	Triphenylphosphine oxide	0.66
			54.521	Triphenylphosphine oxide	4.53	55.834	Phosphine oxide, diphenyl (phenylmethyl)-	0.98
			55.783	Phosphine oxide, diphenyl (phenylmethyl)-	3.60			
			65.997	Heptacosyl acetate	4.50			

propanediyl)bis, 4,4′-(Hexafluoroisopropylidene) diphenol, 1,2-Propanediol, 3-benzyloxy-1,2-diacetyl-, etc. However, styrene represents the main compound with huge abundance estimated at 48.53 % (500 °C), 19.89 % (550 °C), and 29.77 % (600 °C) based on area under the GCMS curves, as illustrated in Table 2. In fact, styrene is the main compound of UPR and is usually used to enhance its thermal resistance and mechanical performance [52,53]. Also, the condensated tar fraction **(**Fig. 4**D-F)** showed almost similar composition to oil with styrene amounting to 44.42 % (500 °C), 32.59 % (550 °C), and 31.65 % (600 °C), as shown in Table 3. As mentioned above, the WTBs feedstock is composed of three major components, GF, UPR, and gelcoat coating layer. Because GF has a higher thermal stability, it can only decompose the organic part, including UPR and coat layer, which is composed of various components such as silicone oil, vinyl monomer, low molecular weight unsaturated polyester and other additives [30,54]. Under the applied pyrolysis temperature all these elements degrade together after breaking down the chemical and friction bonds between them and GF in the dismantling stage [19]. Then, as the reaction temperature increases, more heat flux produces and diffuses into the cross-linked UPR and breaks their molecules into smaller molecules followed by broken down their Van der Waals bonds and polymer chains (including their end chain or random chain scission) into short chain forms [31,38]. The radical of these small molecules were formed and undergoes a condensation reaction and releases some gaseous pieces [17], while styrene compound remaining in the non-condensed part with other GC/MS compounds. It can be collected and used along with pyrolysis oil in different chemical, fuel, and adhesion materials manufacturing fields [54–56]. Similar styrene-rich oil (upto 78.7 wt% styrene) was obtained from the pyrolysis of polystyrene waste, which can be purified and separated in the form of a styrene monomer using vacuum distillation of

Table 3
GC/MS of distribution of condensed tar products recovered at various tempertures.

500 °C			550 °C			600 °C		
Time (min)	GC Compounds	Area (%)	Time (min)	GC Compounds	Area (%)	Time (min)	GC Compounds	Area (%)
2.436	1-Propene, 3,3′-oxybis-	0.62	2.397	1-Propene, 3,3′-oxybis-	0.37	2.436	1-Propene, 3,3′-oxybis-	0.51
2.837	1,3-Dioxolane, 2,2,4-trimethyl-	0.39	3.257	4-Pentenal, 2-methyl-	0.35	3.290	4-Pentenal, 2-methyl-	0.62
3.270	4-Pentenal, 2-methyl-	0.64	3.574	Toluene	7.41	3.619	Toluene	7.32
3.619	Toluene	9.32	4.066	1,3-Dioxolane, 2-ethyl-4-methyl-	1.46	4.124	1,3-Dioxolane, 2-ethyl-4-methyl-	1.91
4.124	1,3-Dioxolane, 2-ethyl-4-methyl-	2.18	4.331	1,3-Dioxolane, 2-ethyl-4-methyl-	0.85	4.376	1,3-Dioxolane, 2-ethyl-4-methyl-	1.00
4.383	1,3-Dioxolane, 2-ethyl-4-methyl-	1.20	5.566	Propane, 1,1′-[ethylidenebis (oxy)] bis-	9.20	5.625	Propane, 2,2′-[ethylidenebis(oxy)] bis-	7.20
5.631	Propane, 2,2′-[ethylidenebis(oxy)] bis-	2.30	6.724	Ethylbenzene	3.16	6.401	1,3-Butanediol, (R)-	1.00
6.375	2-Propanol, 1-(2-propenyloxy)-	1.21	7.921	Styrene	32.59	6.763	Ethylbenzene	4.20
6.757	Ethylbenzene	4.99	8.820	2-Pentanol, 2,3-dimethyl-	26.55	7.080	Thiazole	0.85
7.061	5-Methyltetrahydrofuran-2-methanol,cis & trans	1.10	11.860	.alpha.-Methylstyrene	2.99	7.966	Styrene	31.65
7.979	Styrene	44.42	12.145	Heptane, 2,2,4,6,6-pentamethyl-	1.21	8.872	Hydrazine, 1,1-bis(1-methylethyl)-	26.48
8.872	2-Pentanol, 2,3-dimethyl-	11.22	19.804	Benzoic acid	4.84	9.402	Benzene, (1-methylethyl)-	0.34
9.396	Benzene, (1-methylethyl)-	0.36	24.597	Phthalic anhydride	2.57	10.631	Benzene, propyl-	0.42
10.314	Benzene, cyclopropyl-	0.39	26.544	Biphenyl	0.56	11.058	Benzaldehyde	0.33
10.625	Benzene, propyl-	0.36	29.145	Dimethyl phthalate	0.38	11.854	.alpha.-Methylstyrene	4.28
10.968	Benzaldehyde	0.62	34.623	Benzene, 1,1′-(1,3-propanediyl)bis	2.77	12.171	Heptane, 2,2,4,6,6-pentamethyl-	1.41
11.841	.alpha.-Methylstyrene	5.36	36.486	N-Benzyl-1 H-benzimidazole	0.56	13.704	Benzene, 1-ethenyl-2-methyl-	0.44
12.177	Decane, 2,2-dimethyl-	1.90	36.881	1,2-Diphenylcyclopropane	0.38	16.919	1-Butanamine, N-methyl-N-nitro-	0.55
13.672	Benzene, cyclopropyl-	0.71	49.385	Butanal, dimethylhydrazone	0.34	19.752	Benzoic acid	0.59
14.364	Benzene, 3-butenyl-	0.39	52.956	3-Phenylthiane,S-oxide	1.47	29.048	Dimethyl phthalate	0.81
14.571	1-Propanol, 2-(2-hydroxypropoxy)-	0.66				34.611	Benzene, 1,1′-(1,3-propanediyl)bis	3.54
19.675	Benzoic acid	1.02				34.837	1,2-Benzenedicarboxylic acid, monobutyl ester	0.97
26.454	Biphenyl	0.85				36.849	1,2-Diphenylcyclopropane	0.54
29.009	Dimethyl phthalate	2.22				39.093	Pentadecanal-	0.59
34.604	Benzene, 1,1′-(1,3-propanediyl)bis	3.21				44.055	17-Octadecenal	0.40
36.461	Benzene, 6-heptynyl-	0.99				44.883	4,4′-(Hexafluoroisopropylidene) diphenol	0.43
36.842	1,2-Diphenylcyclopropane	0.68				46.377	Octadecanal	0.35
44.844	4,4′-(Hexafluoroisopropylidene) diphenol	0.68				48.609	Pentadecanal-	0.34
						54.560	Triphenylphosphine oxide	0.36
						55.828	Phosphine oxide, diphenyl (phenylmthyl)-	0.54

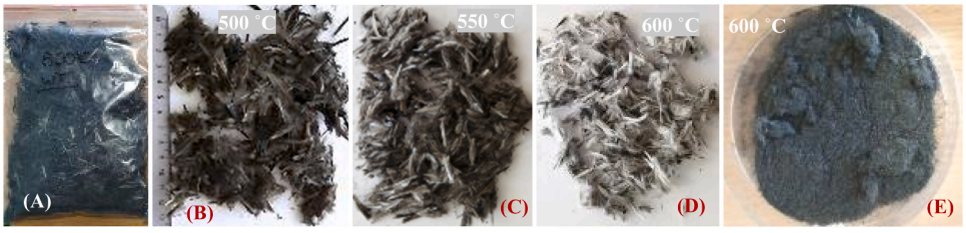

Fig. 5. A) solid residual product, B-D) images of the liberated fibres from solid residual product at 500, 550, and 600°C, respectively and E) char fraction at 600°C.

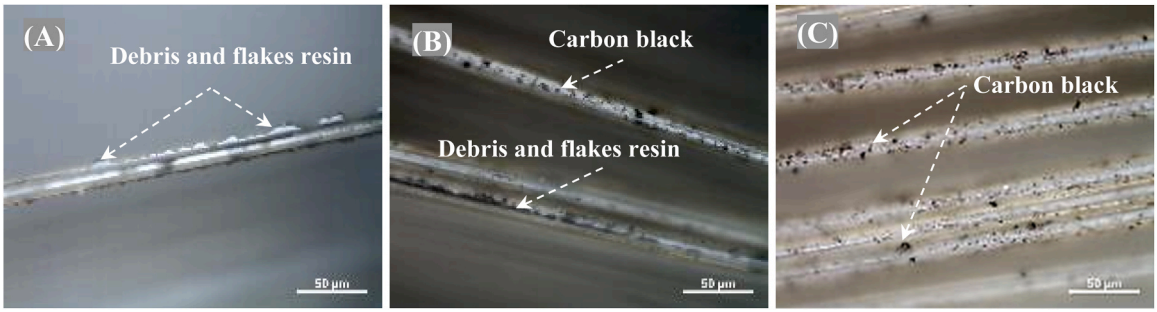

Fig. 6. Optical images of the recovered glass fibres at A) 500, B) 550, and C) 600°C.

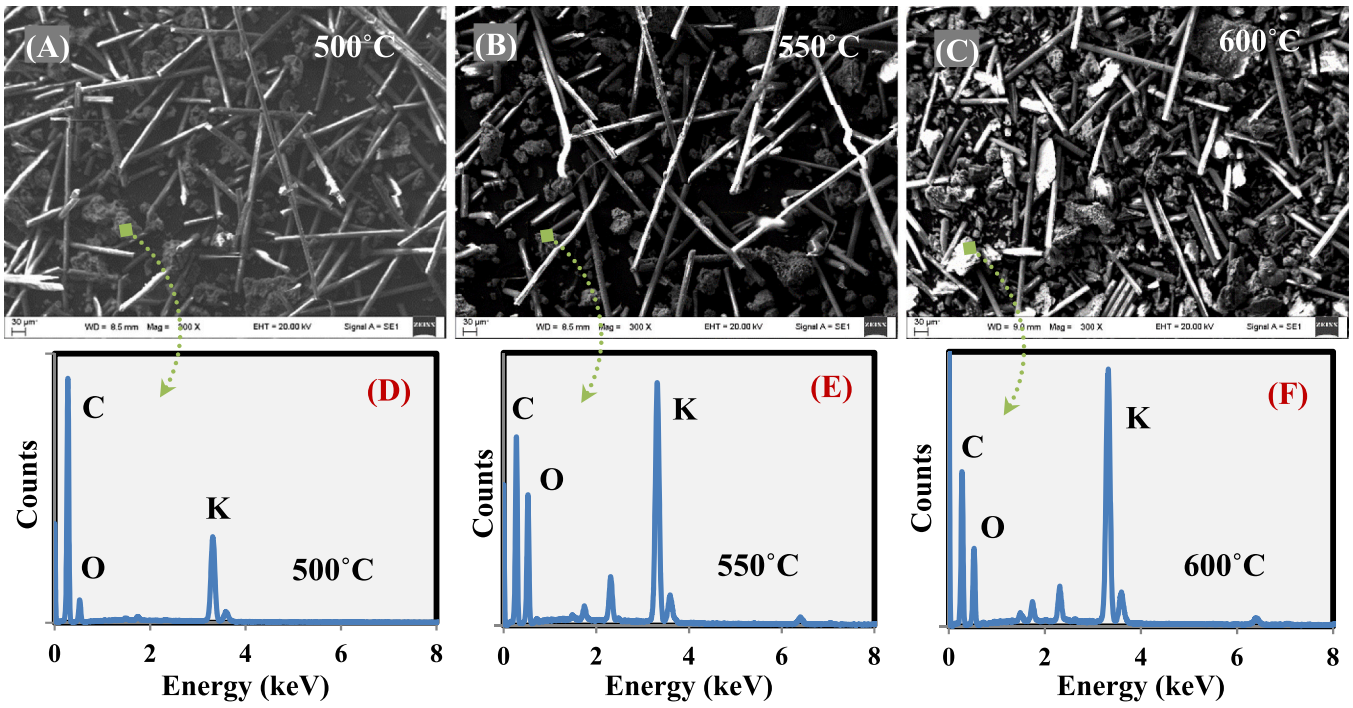

Fig. 7. A-C) SEM images of the obtained char products and D-F) EDX images of the obtained char product at 500, 550, and 600°C, respectively.

Table 4
EDX elemental analysis of the undecomposed debris particles.

Element (wt%)	500 °C	550 °C	600 °C
Carbon	63.88	33.98	34.84
Oxygen	20.84	41.66	33.88
Potassium	14.89	19.59	25.51
Silicon	0.25	0.54	0.96
Aluminium	0.14	——	0.51
Iron	——	1.95	2.06
Sulfur	——	2.27	2.25

the pyrolysis oil that can be repolymerized into a latex fraction or other polymeric materials [57]. Accordingly, 500 °C is the most suitable temperature for processing of WTBs with a high recovery rate for styrene-rich oil and styrene-rich tar.

3.4. Analysis of solid residual products

The solid residual products obtained from pyrolysis of WTBs had two fractions with different structures and sizes, as shown in Fig. 5**A**. One of them was distinguished by its thin filaments of a few millimetres in length referring to fibres, while the other part was in the form of powder referring to a char component. These two fractions were separated using a sieving process following by washing of the liberated fibres using deionized water. Fig. 5**B-D** shows the images of the liberated fibres at 500, 550, and 600°C, respectively. As shown, the fibres recovered at 500 °C were completely black, and later they turned almost gray and white at 550 °C and 600 °C, respectively. The separate char was in a powder shape contaminated with a very short fibre, as shown in Fig. 5**E**. The virtual shapes for the other batches (500 °C and 550 °C) was nearly the same. Both fractions (fibres and char) were analyzed using SEM-EDX, an optical microscope, and FTIR analysis to check effect of pyrolysis temperature on their structure and morphology.

Fig. 6 shows optical microscope photos of the liberated fibres received at 500, 550, and 600 °C, respectively. The optical images showed thin filaments of a few millimetres in length contaminated on their surface with some debris and flakes left from the resin portion. Some black dots manifest deposition of char (black carbon) and adhesion by a strong mechanical bond that cannot be easily separated, thus further treatment is required [58]. These debris and flakes decrease gradually with increase in temperature. The resin chains break down

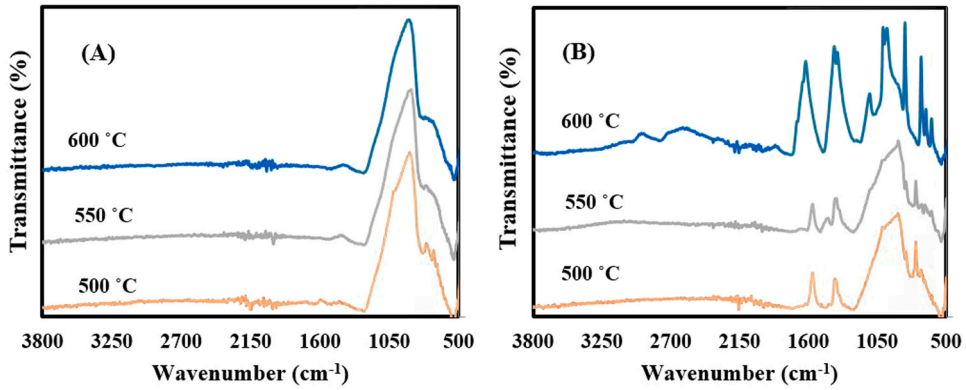

Fig. 8. FTIR analysis of the A) fibres and B) chars liberated at various temperatures.

Fig. 9. Circular economy of wind energy based on the suggested recycling strategy of WTBs.

and overcome their Van der Waals bonds, which helps to achieve complete decomposition of resin and its separation from fibres surfaces [59,60]. Meanwhile, the intensity of the black dots did not change much even with increase in temperature. Thus, a post-oxidation process or chemical treatment with solvents is highly recommended to remove residual organic compounds from the recovered fibres and make them purer [61,62]. The SEM images **(**Fig. 7**A-C)** of the char fraction showed that it consisted of particles in the form of irregular debris accompanied by microfibers. The surfaces of these microfibers became more visible at elevated temperatures and these results match with those obtained from the optical results. Also, the size and shape of these particles and debris became smoother with increase of temperature due to surface treatment of functionalized particles [63,64].

The EDX measurements (Fig. 7**D-F)** showed that carbon and oxygen were the main elements in the undecomposed debris particles up to 64 wt%, as illustrated in Table 4, where these elements represent the major elements in all organic compounds [65]. Also, potassium element was strongly present in the undecomposed debris particles in the ranges of 14.9 wt% (500°C) and 25.5 wt% (600°C). Although potassium is not a typical or primary element in the composition of wind turbine blades components (fibres, resin, coat layer, etc.), however this element may be generated from other natural sources during the operation time, such as rocks, soils, and organic matter [66]. Actually, potassium is not a common element in either GF or UPR. However, potassium element is derived from UPR systems, which are typically a mixture of unsaturated polyester resin, crosslinking agent, and various additives to improve their properties and helps initiate the curing process. Potassium compounds, such as potassium hydroxide (KOH) one of these additives that is widely used as a catalyst or a curing agent in resin systems for hardening and producing a strong matrix [67,68]. In addition, low concentration of other elements (silicon, aluminium, iron, and sulfur) was observed in fibreglass, resin components, and in a coat layer [59,69,70]. Based on the EDX results, this type of char can be defined as a potassium-rich char with high potential applications in various fields, for example, adsorption and fertilizing after being separating from microfibres [71,72].

Fig. 8 shows FTIR spectrum of the fibres and chars liberated from pyrolysis of WTBs under various temperatures. The FTIR analysis of fibres **(**Fig. 8**A)** shows similar spectra even with changing pyrolysis temperature with sharp peak at 913 cm^{-1} due to Si-O-Si bond and this is a typical structure of fibreglass [73]. Meanwhile, FTIR of powder fraction showed several functional groups at 742 cm^{-1} (aromatic nucleus CH, three-to-four adjacent H deformation), 875 cm^{-1} (calcium carbonate), 1375 cm^{-1} (aliphatic chains CH3–,CH2–), and 1562 cm^{-1} (conjugated aromatic ring stretching C═C) and this is a typical structure of char product combined with some fibres [74,75]. As shown, the intensity of these peaks decreased with increase in the pyrolysis temperature leading to decrease in the degree of polymerization [76].

3.5. Integration of WTBs into circular economy and their contribution to sustainability of resin and fibres

Recycling of WTBs represents the main obstacle in converting wind energy into an integrated green approach, without which it is classified as a green technology of the operational period, and afterwards it remains a great challenge for this sector with regard to its integration into the circular economy system and closing of its loop [77]. With reference to the proposed approach to WTBs and their output products and boundaries, this pyrolysis treatment can help a lot to achieve this, as its infrastructure is widely available in the European Union, and currently there are many startups and pyrolysis projects in advanced stages that would help in its implementation [78], where the necessary capabilities are available to collect the WTBs and separate them from other turbine components without the need for future sorting. Likewise, pretreatment to reduce volume of waste including WTBs and facilitate reactor feed is widely available. All these operations and transportation are carried out by specialized companies, which ensure performance and implementation of this strategy to the fullest without the need to add any infrastructure and economic burdens [79]. Once the milled WTBs reach the pyrolysis plant, they are directly fed into the reactor under the optimal treatment conditions (500°C), where the resin fraction can be thermally decomposed into oil and carbon black with almost no gas. This oil can be used as a fuel directly or styrene compound may be separated and used in chemical industries, while the potassium-rich char product can be used as an adsorbent, filler material or as a catalyst for NOx reduction after modification [74]. Meanwhile, the fibre remains a final product without any degeneration, as shown in Fig. 9. The reclaimed GF can be used as a filler material in composite and building materials after modifying their surface to improve their compatibility. Accordingly, this strategy can help to close and generalize the circular economic aspect to ensure that wind energy is converted into a green, renewable resource and that any related environmental concerns are removed.

4. Conclusions

In this work, the thermochemical performance of commercial WTBs (GF/UPR) was studied in the present research in a pyrolysis plant with 250 g at 500, 550, and 600°C to recover styrene and to maximize the role of the recovered GF. The basic properties of the recovered energy products and liberated fibreglass and char were analyzed using GC/MS, FTIR, SEM-EDX, and an optical microscope. The results revealed that the UPR part can decompose only to styrene (48.53 %) -rich oil product with yield of 44.5 wt% at 500°C without almost any gaseous products. However, the surfaces of the reclaimed GF became more visible at the highest temperature (600°C) based on SEM analysis. The formulated char product was very rich in potassium (25.5 wt% at 600 °C) and became smoother and more uniform at the elevated temperatures. This char can be used as a catalyst for NOx reduction with the help of oxygen. Based on that, pyrolysis process has a high potential in treatment of millions of tonnes of WTBs, especially which has GF/UPR structure without producing almost any gaseous product. However, the liberated GF still needs post-oxidation process or chemical treatment to remove any undecomposed compounds making them more visible. Also, techno-economic analysis of suggested approach is highly recommended to evaluate accurate price of the recovered products and economic performance of all processes (including pretreament and treatment) and the

amount of waste that can be recycled with high return.

CRediT authorship contribution statement

Samy Yousef: Conceptualization, Data curation, Formal analysis, Funding acquisition, Investigation, Methodology, Project administration, Resources, Software, Supervision, Writing—original draft, Writing—review & editing. **Justas Eimontas**: Conceptualization, Data curation, Formal analysis. **Kęstutis Zakarauskas:** Conceptualization, Data curation, Formal analysis. **Nerijus Striūgas**: Conceptualization, Data curation, Formal analysis.

Declaration of Competing Interest

The authors declare that they have no known competing financial interests or personal relationships that could have appeared to influence the work reported in this paper.

Data availability

The data that has been used is confidential.

Acknowledgment

This project has received funding from the Research Council of Lithuania (LMTLT), agreement No. S-MIP-23-118.

References

[1] C.W. Su, K. Khan, M. Umar, W. Zhang, Does renewable energy redefine geopolitical risks, Energy Policy (2021), https://doi.org/10.1016/j.enpol.2021.112566.
[2] V. Battaglia, G. De Luca, S. Fabozzi, H. Lund, L. Vanoli, Integrated energy planning to meet 2050 European targets: a Southern Italian region case study, Energy Strategy Rev. (2022), https://doi.org/10.1016/j.esr.2022.100844.
[3] P. Majewski, N. Florin, J. Jit, R.A. Stewart, End-of-life policy considerations for wind turbine blades, Renew. Sustain. Energy Rev. (2022), https://doi.org/10.1016/j.rser.2022.112538.
[4] M.Y. Khalid, Z.U. Arif, M. Hossain, R. Umer, Recycling of wind turbine blades through modern recycling technologies: a road to zero waste, Renew. Energy Focus (2023), https://doi.org/10.1016/j.ref.2023.02.001.
[5] Amrit Shankar Verma, Jiquan Yan, Weifei Hu, Zhiyu Jiang, Wei Shi, Julie J. E. Teuwen, A review of impact loads on composite wind turbine blades: impact threats and classification, Renew. Sustain. Energy Rev. (2023), https://doi.org/10.1016/j.rser.2023.113261.
[6] M. Rani, P. Choudhary, V. Krishnan, S. Zafar, A review on recycling and reuse methods for carbon fiber/glass fiber composites waste from wind turbine blades, Compos. Part B: Eng. (2021), https://doi.org/10.1016/j.compositesb.2021.108768.
[7] M.J. Leon, Recycling of wind turbine blades: recent developments, Curr. Opin. Green. Sustain. Chem. (2023), https://doi.org/10.1016/j.cogsc.2022.100746.
[8] P.S. Oliveira, M.L.P. Antunes, N.C. da Cruz, E.C. Rangel, A.R.G. de Azevedo, S. F. Durrant, Use of waste collected from wind turbine blade production as an eco-friendly ingredient in mortars for civil construction, J. Clean. Prod. (2020), https://doi.org/10.1016/j.jclepro.2020.122948.
[9] A. Yazdanbakhsh, L.C. Bank, K.A. Rieder, Y. Tian, C. Chen, Concrete with discrete slender elements from mechanically recycled wind turbine blades, Resour., Conserv. Recycl. (2018), https://doi.org/10.1016/j.resconrec.2017.08.005.
[10] M. Tatariants, G. Denafas, R. Bendikiene, Separation and purification of metal and fiberglass extracted from waste printed circuit boards using milling and dissolution techniques, Environ. Prog. Sustain. Energy 37 (6) (2018) 2082–2092, https://doi.org/10.1002/ep.12899.
[11] Circular economy performance and carbon footprint of wind turbine blade waste management alternatives
[12] R. Fonte, G. Xydis, Wind turbine blade recycling: an evaluation of the European market potential for recycled composite materials, J. Environ. Manag. (2021), https://doi.org/10.1016/j.jenvman.2021.112269.
[13] M. Tatariants, R. Bendikiene, R. Kriūkienė, G. Denafas, A new industrial technology for closing the loop of full-size waste motherboards using chemical-ultrasonic-mechanical treatment, Process Saf. Environ. Prot. 140 (2020) 367–379, https://doi.org/10.1016/j.psep.2020.04.002.
[14] Mumtaz Hamza, Sobek Szymon, Sajdak Marcin, Muzyka Roksana, Drewniak Sabina, Werle Sebastian, Oxidative liquefaction as an alternative method of recycling and the pyrolysis kinetics of wind turbine blades, Energy (2023), https://doi.org/10.1016/j.energy.2023.127950.
[15] I. Stasiulaitiene, K. Zakarauskas, N. Striūgas, An eco-friendly strategy for recovery of H2-CH4-rich syngas, benzene-rich tar and carbon nanoparticles from surgical mask waste using an updraft gasifier system, Energy Sources, Part A: Recov. Util., Environ. Eff. (2023), https://doi.org/10.1080/15567036.2023.2207507.
[16] J. Chen, T. Meng, Q. Wang, Y. Bai, E. Jiaqiang, E. Leng, F. Zhang, G. Liao, Study on the mechanisms of epoxy resin gasification in supercritical water by molecular dynamics and experimental methods, Chem. Eng. J. (2022), https://doi.org/10.1016/j.cej.2021.133828.
[17] Ming-xin Xu, Hai-wen Ji, Ya-chang Wu, Jin-yi Di, Xiang-xi Meng, Hao Jiang, Qiang Lu, The pyrolysis of end-of-life wind turbine blades under different atmospheres and their effects on the recovered glass fibers, Compos. Part B: Eng. (2023), https://doi.org/10.1016/j.compositesb.2022.110493.
[18] S. Yousef, J. Eimontas, N. Striūgas, M. Praspaliauskas, M.A. Abdelnaby, Pyrolysis kinetic behaviour of glass fibre-reinforced epoxy resin composites using linear and nonlinear isoconversional methods, Polymers 13 (10) (2021), https://doi.org/10.3390/polym13101543.
[19] J. Eimontas, N. Striūgas, S.P. Subadra, M.A. Abdelnaby, Thermal degradation and pyrolysis kinetic behaviour of glass fibre-reinforced thermoplastic resin by TG-FTIR, Py-GC/MS, linear and nonlinear isoconversional models, J. Mater. Res. Technol. 15 (2021) 5360–5374, https://doi.org/10.1016/j.jmrt.2021.11.011.
[20] L. Ge, X. Li, H. Feng, Chunyao Xu, Y. Lu, B. Chen, D. Li, Chang Xu, Analysis of the pyrolysis process, kinetics and products of the base components of waste wind turbine blades (epoxy resin and carbon fiber, J. Anal. Appl. Pyrolysis (2023), https://doi.org/10.1016/j.jaap.2023.105919.
[21] L. Ge, Chunyao Xu, H. Feng, H. Jiang, X. Li, Y. Lu, B. Chen, Chang Xu, Study on isothermal pyrolysis and product characteristics of basic components of waste wind turbine blades, SSRN Electron. J. (2023), https://doi.org/10.2139/ssrn.4341317.
[22] W. Chen, M. Ye, M. Li, B. Xi, J. Hou, X. Qi, J. Zhang, Y. Wei, F. Meng, Characteristics, kinetics and product distribution on pyrolysis process for waste wind turbine blades, J. Anal. Appl. Pyrolysis (2023), https://doi.org/10.1016/j.jaap.2023.105859.
[23] X. Xiong, L. Li, F. Chen, J. Zhang, H. Tan, Typical pollutant species evolution behaviors study in retired wind turbine blade and coal thermal conversion process, J. Anal. Appl. Pyrolysis (2022), https://doi.org/10.1016/j.jaap.2022.105771.
[24] I. Kiminaitė, J. Eimontas, N. Striūgas, M.A. Abdelnaby, Catalytic pyrolysis kinetic behaviour of glass fibre-reinforced epoxy resin composites over ZSM-5 zeolite catalyst, Fuel (2022), https://doi.org/10.1016/j.fuel.2022.123235.
[25] Ieva Kiminaitė, Justas Eimontas, Nerijus Striūgas, Mohammed Ali Abdelnaby, Recovery of phenol and acetic acid from glass fibre reinforced thermoplastic resin using catalytic pyrolysis process on ZSM-5 zeolite catalyst and its kinetic behaviour, Thermochim. Acta (2022), https://doi.org/10.1016/j.tca.2022.179293.
[26] J. Eimontas, N. Striūgas, et al., Catalytic pyrolysis and kinetic study of glass fibre-reinforced epoxy resin over CNTs, graphene and carbon black particles/ZSM-5 zeolite hybrid catalysts, J. Therm. Anal. Calor. 148 (2023) 897–912, https://doi.org/10.1007/s10973-022-11776-9.
[27] J. Eimontas, I. Stasiulaitiene, K. Zakarauskas, N. Striūgas, Pyrolysis of all layers of surgical mask waste as a mixture and its life-cycle assessment, Sustain. Prod. Consum. 32 (2022) 519–531, https://doi.org/10.1016/j.spc.2022.05.011.
[28] V. Lekavičius, N. Striūgas, Techno-economic analysis of thermochemical conversion of waste masks generated in the EU during COVID-19 pandemic into energy products, Energies 16 (2023) 3948, https://doi.org/10.3390/en16093948.
[29] Mohammad Amin Mousavi Khorasani, Samaneh Sahebian, Ahad Zabett, Effects of toughened polyester on fatigue behavior of glass fiber reinforced polyester composite for wind turbine blade, Polym. Compos. (2020), https://doi.org/10.1002/pc.25808.
[30] L. Mishnaevsky, K. Branner, H.N. Petersen, J. Beauson, M. McGugan, B.F. Sørensen, Materials for wind turbine blades: an overview, Materials 10 (2017) 1285, https://doi.org/10.3390/ma10111285.
[31] Baolong Wang, Xinyu Wang, Ningdi Xu, Yibo Shen, Fei Lu, Yingying Liu, Yudong Huang, Zhen Hu, Recycling of carbon fibers from unsaturated polyester composites via a hydrolysis oxidation synergistic catalytic strategy, Compos. Sci. Technol. (2021), https://doi.org/10.1016/j.compscitech.2020.108589.
[32] European chemicals agency: Styrene infocard. https://www.e cha.europa.eu/substance-information/-/substanceinfo/100.00 2.592.
[33] J. Huff, P.F. Infante, Styrene exposure and risk of cancer, Mutagenesis 26 (5) (2011) 583–584.
[34] https://www.reinforcedplastics.com/content/features/recycling-wind/.
[35] Xiong-lei Wang, et al., High-efficiency hydrolysis of thermosetting polyester resins into porous functional materials using low-boiling aqueous solvents, ACS Sustain. Chem. Eng. 8 (2020) 16010–16019.
[36] G. Crini, E. Lichtfouse, Advantages and disadvantages of techniques used for wastewater treatment, Environ. Chem. Lett. 17 (2019) 145–155, https://doi.org/10.1007/s10311-018-0785-9.
[37] Y. Bautista, A. Gozalbo, S. Mestre, V. Sanz, Thermal degradation mechanism of a thermostable polyester stabilized with an open-cage oligomeric silsesquioxane, Materials (2017) 11.
[38] Khedoudja Laoubi, et al., Thermal behavior of E-glass fiber-reinforced unsaturated polyester composites, Compos. Part B-Eng. 56 (2014) 520–526.
[39] B. Kjærside Storm, Surface protection and coatings for wind turbine rotor blades, Adv. Wind Turbine Bl. Des. Mater. (2013), https://doi.org/10.1533/9780857097286.3.387.
[40] I.B.C.M. Rocha, S. Raijmaekers, R.P.L. Nijssen, F.P. van der Meer, L.J. Sluys, Hygrothermal ageing behaviour of a glass/epoxy composite used in wind turbine blades, Compos. Struct. (2017), https://doi.org/10.1016/j.compstruct.2017.04.028.
[41] J.I. Bech, N.F.-J. Johansen, M.B. Madsen, Á. Hannesdóttir, C.B. Hasager, Experimental study on the effect of drop size in rain erosion test and on lifetime

prediction of wind turbine blades, SSRN Electron. J. (2022), https://doi.org/10.2139/ssrn.4011160.
[42] J.Sebastian Arrieta, Richaud Emmanuel, Fayolle Bruno, Nizeyimana Fidèle, Thermal oxidation of vinyl ester and unsaturated polyester resins, Polym. Degrad. Stab. 129 (2016) 142–155.
[43] P. Liu, F. Meng, C.Y. Barlow, Wind turbine blade end-of-life options: an economic comparison, Resour., Conserv. Recycl. (2022), https://doi.org/10.1016/j.resconrec.2022.106202.
[44] I. Crespo, J. Hertzog, V. Carré, F. Aubriet, B. Valle, Alumina-embedded Hzsm-5 with enhanced behavior for the catalytic cracking of biomass pyrolysis bio-oil: insights into the role of mesoporous matrix in the deactivation by coke, SSRN Electron. J. (2023), https://doi.org/10.2139/ssrn.4374512.
[45] Justas Eimontas, Nerijus Striūgas, Alaa Mohamed, Marius Praspaliauskas, Mohammed Ali Abdelnaby, Phenol and benzoic acid recovery from end-of-life of polysulfone ultrafiltration membranes and its thermochemical kinetic behaviour, Energy Sources, Part A: Recov. Util., Environ. Eff. 45 (2) (2023) 6043–6061, https://doi.org/10.1080/15567036.2023.2213669.
[46] J. Eimontas, N. Striūgas, M.A. Abdelnaby, Influence of carbon black filler on pyrolysis kinetic behaviour and TG-FTIR-GC–MS analysis of glass fibre reinforced polymer composites, Energy (2021), https://doi.org/10.1016/j.energy.2021.121167.
[47] K. Zakarauskas, J. Eimontas, N. Striūgas, Microcrystalline paraffin wax, biogas, carbon particles and aluminum recovery from metallised food packaging plastics using pyrolysis, mechanical and chemical treatments, J. Clean. Prod. (2021), https://doi.org/10.1016/j.jclepro.2021.125878.
[48] N. Striūgas, J. Eimontas, K. Zakarauskas, A. Mohamed, A new strategy for using lint-microfibers generated from clothes dryer as a sustainable source of renewable energy, Sci. Total Environ. (2021), https://doi.org/10.1016/j.scitotenv.2020.143107.
[49] Xiaoxiao Zhang, et al., Effect of pyrolysis temperature and correlation analysis on the yield and physicochemical properties of crop residue biochar, Bioresour. Technol. 296 (2019), 122318.
[50] S. Yousef, J. Eimontas, K. Zakarauskas, N. Striūgas, A new sustainable strategy for oil, CH4 and aluminum recovery from metallised food packaging plastics waste using catalytic pyrolysis over ZSM-5 zeolite catalyst, Thermochim. Acta (2022), https://doi.org/10.1016/j.tca.2022.179223.
[51] M.A. Abdelnaby, J. Eimontas, N. Striūgas, A new strategy for butanol extraction from COVID-19 mask using catalytic pyrolysis process over ZSM-5 zeolite catalyst and its kinetic behavior, Thermochim. Acta (2022), https://doi.org/10.1016/j.tca.2022.179198.
[52] E.M.S. Sanchez, C.A.C. Zavaglia, M.I. Felisberti, Unsaturated polyester resins: Influence of the styrene concentration on the miscibility and mechanical properties, Polymer (2000), https://doi.org/10.1016/S0032-3861(99)00184-6.
[53] S. Cousinet, A. Ghadban, E. Fleury, F. Lortie, J.P. Pascault, D. Portinha, Toward replacement of styrene by bio-based methacrylates in unsaturated polyester resins, Eur. Polym. J. (2015), https://doi.org/10.1016/j.eurpolymj.2015.02.016.
[54] D. Rubeš, J. Vinklárek, L. Prokůpek, Š. Podzimek, J. Honzíček, Styrene-free unsaturated polyester resins derived from itaconic acid curable by cobalt-free accelerators, J. Mater. Sci. 58 (2023) 6203–6219.
[55] Roshi Dahal, Petri Uusi-Kyyny, Juha-Pekka Pokki, Taina Ohra-aho, Ville Alopaeus, Conceptual design of a distillation process for the separation of styrene monomer from polystyrene pyrolysis oil: experiment and simulation, Chem. Eng. Res. Des. (2023), https://doi.org/10.1016/j.cherd.2023.05.039.
[56] E.M.S. Sanchez, C.A.C. Zavaglia, M.I. Felisberti, Unsaturated polyester resins: Influence of the styrene concentration on the miscibility and mechanical properties, Polymer (2000), https://doi.org/10.1016/S0032-3861(99)00184-6.
[57] R. Dahal, P. Uusi-Kyyny, J. Pokki, T. Ohra-Aho, V. Alopaeus, Conceptual design of a distillation process for the separation of styrene monomer from polystyrene pyrolysis oil: experiment and simulation, Chem. Eng. Res. Des. (2023).
[58] N. Striūgas, J. Eimontas, S.P. Subadra, Functionalization of char derived from pyrolysis of metallised food packaging plastics waste and its application as a filler in fiberglass/epoxy composites, Process Saf. Environ. Prot. (2021), https://doi.org/10.1016/j.psep.2021.01.009.
[59] P. Broøndsted, R.P.L. Nijssen, Advances in wind turbine blade design and materials, Adv. Wind Turbine Bl. Des. Mater. (2013), https://doi.org/10.1533/9780857097286.
[60] M. Tichonovas, M. Tatariants, L. Kliucininkas, S.I. Lukošiūtė, L. Yan, Sustainable green technology for recovery of cotton fibers and polyester from textile waste, J. Clean. Prod. (2020), https://doi.org/10.1016/j.jclepro.2020.120078.
[61] H. Li, N. Wang, X. Han, H. Yuan, J. Xie, Mechanism identification and kinetics analysis of thermal degradation for carbon fiber/epoxy resin, Polymers (2021), https://doi.org/10.3390/polym13040569.
[62] M. Tatariants, M. Tichonovas, Z. Sarwar, I. Jonuškienė, L. Kliucininkas, A new strategy for using textile waste as a sustainable source of recovered cotton, Resour. Conserv. Recycl. (2019), https://doi.org/10.1016/j.resconrec.2019.02.031.
[63] R. Kalpokaitė-Dičkuvienė, A. Baltušnikas, I. Pitak, S.I. Lukošiūtė, A new strategy for functionalization of char derived from pyrolysis of textile waste and its application as hybrid fillers (CNTs/char and graphene/char) in cement industry, J. Clean. Prod. (2021), https://doi.org/10.1016/j.jclepro.2021.128058.
[64] E. Trofimov, J. Eimontas, N. Striūgas, M. Hamdy, M.A. Abdelnaby, Conversion of end-of-life cotton banknotes into liquid fuel using mini-pyrolysis plant, J. Clean. Prod. (2020), https://doi.org/10.1016/j.jclepro.2020.121612.
[65] S. Liu, L. Xiao, G. Wang, G. Liu, Y. Mo, W. Lu, Heteroatom-doped carbon materials from bimetal covalent organic polymers as efficient bifunctional electrocatalysts in oxygen reduction and oxygen evolution reactions, Mater. Today Sustain. (2023), https://doi.org/10.1016/j.mtsust.2023.100389.
[66] S.M. Yahaya, A.A. Mahmud, M. Abdullahi, A. Haruna, Recent advances in the chemistry of N, P, K as fertilizer in soil – a review, Pedosphere (2022), https://doi.org/10.1016/j.pedsph.2022.07.012.
[67] J. Liu, K. Wang, L.L. Ma, T. Tang, Insight into the role of potassium hydroxide for accelerating the degradation of anhydride-cured epoxy resin in subcritical methanol, J. Supercrit. Fluids 107 (2016) 605–611.
[68] M.H. Fasihnikoutalab, S. Pourakbar, R.J. Ball, B.B. Huat, The effect of olivine content and curing time on the strength of treated soil in presence of potassium hydroxide, Int. J. Geosynth. Ground Eng. 3 (2017) 1–10.
[69] S.P. Subadra, P. Griskevicius, S. Yousef, Low velocity impact and pseudo-ductile behaviour of carbon/glass/epoxy and carbon/glass/PMMA hybrid composite laminates for aircraft application at service temperature, Polym. Test. (2020), https://doi.org/10.1016/j.polymertesting.2020.106711.
[70] A. Perrot, J. Hyršl, J. Bandžuch, S. Wañousová, J. Hájek, J. Jenčík, T. Herink, A comparative study of a modified unsaturated polyester resin with dicyclopentadiene and methyl dicyclopentadiene blends, Polymer (2023), https://doi.org/10.1016/j.polymer.2022.125639.
[71] Honggang Fan, Jing Gu, Yazhuo Wang, Haoran Yuan, Yong Chen, Bo Luo, Effect of potassium on the pyrolysis of biomass components: pyrolysis behaviors, product distribution and kinetic characteristics, Waste Manag. (2021), https://doi.org/10.1016/j.wasman.2020.12.023.
[72] M.Z. Hossain, M.M. Bahar, B. Sarkar, et al., Biochar and its importance on nutrient dynamics in soil and plant, Biochar 2 (2020) 379–420, https://doi.org/10.1007/s42773-020-00065-z.
[73] S.P. Subadra, S. Tuckute, A. Baltušnikas, S.I. Lukošiūtė, E.L. Arafa, A. Mohamed, Finite element analysis of fibreglass and carbon fabrics reinforced polyethersulfone membranes, Mater. Today Commun. (2022), https://doi.org/10.1016/j.mtcomm.2022.103682.
[74] M.J. Illán-Gómez, C. De Salinas-Martínez Lecea, A. Linares-Solano, L.R. Radovic, Potassium-containing coal chars as catalysts for NOx reduction in the presence of oxygen, Energy Fuels (1998), https://doi.org/10.1021/ef980067w.
[75] J. Eimontas, N. Striūgas, A. Mohamed, M.A. Abdelnaby, Morphology, compositions, thermal behavior and kinetics of pyrolysis of lint-microfibers generated from clothes dryer, J. Anal. Appl. Pyrolysis (2021), https://doi.org/10.1016/j.jaap.2021.105037.
[76] Y. Zhao, D. Feng, Y. Zhang, Y. Huang, S. Sun, Effect of pyrolysis temperature on char structure and chemical speciation of alkali and alkaline earth metallic species in biochar, Fuel Process. Technol. (2016), https://doi.org/10.1016/j.fuproc.2015.06.029.
[77] W. Yang, K.H. Kim, J. Lee, Upcycling of decommissioned wind turbine blades through pyrolysis, J. Clean. Prod. (2022), https://doi.org/10.1016/j.jclepro.2022.134292.
[78] https://www.plasteurope.com/news/ITERO_t246832/.
[79] https://orsted.com/en/media/newsroom/news/2021/06/702084352457649.